Microchemical Journal 210 (2025) 112971

Contents lists available at ScienceDirect

Microchemical Journal

journal homepage: www.elsevier.com/locate/microc

Advancing preservation: a chemometric approach for monitoring the degradation of protective coatings for bronze statues

Giulia Pellis [a], Maxim Tiburziano [b], Barbara Giussani [b,*], Paola Letardi [c], Barbara Salvadori [d], Antonio Sansonetti [e], Dominique Scalarone [a]

[a] Department of Chemistry University of Torino Via Pietro Giuria 7 Torino Italy
[b] Science and High Technology Department Università degli Studi dell'Insubria Via Valleggio 9 Como Italy
[c] Institute of Anthropic Impacts and Sustainability in the Marine Environment CNR Via De Marini 6 Genova Italy
[d] Institute of Heritage Science CNR Via Madonna del Piano 10 Sesto Fiorentino Italy
[e] Institute of Heritage Science CNR Via Roberto Cozzi 53 Milan Italy

ARTICLE INFO

Keywords:
Decay studies
Protective coatings
Applied chemometrics
PCA
Sustainable studies

ABSTRACT

Bronze outdoor statues are often covered by a corrosion patina that forms due to environmental exposure, providing both aesthetic value and, partly, a surface passivation. However, this patina does not prevent from decay by external factors such as pollution, UV radiation, and humidity. To mitigate these decay processes, protective coatings are commonly used, but existing solutions often have drawbacks related to health, durability, and the need for frequent reapplication. The development of reliable, long-term conservation methods is essential. This work focuses on evaluating coatings formulated with Paraloid® B44, incorporating non-toxic corrosion inhibitors and light stabilizers. A total of twenty-one coatings were subjected to accelerated aging with artificial sunlight, and their decay was monitored using a multi-analytical approach involving Fourier Transform Infrared Spectroscopy (FT-IR) and UV–Vis spectroscopy, both with benchtop and portable spectrometers. The aim is to propose a method that combines spectroscopic data with chemometrics, specifically Principal Component Analysis (PCA), to objectively assess coating decay over time. The results demonstrate that PCA provides a simple yet powerful tool to distinguish between different formulations, track their aging, and rationalize decay processes. This approach not only facilitates the comparative analysis of coatings but also holds potential for field applications using portable instruments. By integrating spectroscopy with chemometrics, this method aligns with the principles of green analytical chemistry, offering a non-invasive, efficient means to monitor the effectiveness of protective coatings for cultural heritage preservation.

1. Introduction

Bronze outdoor statues often display a corrosion patina due to environmental exposure. This patina plays an important aesthetic and passivation role on the surface; however, it does not hamper decay processes promoted by light, oxygen, pollution and humidity [1]. To slow down these disfiguring processes protective coatings are applied. However, the most commonly used ones have several drawbacks related to health and durability and need to be replaced [2]. The development of safe and reliable long-term methods and strategies for the conservation of these artworks is nowadays a mandatory prerequisite [3,4].

A wide variety of materials have been developed so far, including organic coatings based on organosilanes [5–7], fluoropolymers [8,9], acrylic resins [10–12], cellulose nitrate [13], natural or synthetic waxes (with or without corrosion inhibitors) [14,15]. Moreover, different techniques and aging methods have been proposed in the literature, with many attempts to make a complex comparison between them. The typical approach involves aging the coatings either through accelerated or natural methods and monitoring their decay using a multi-analytical approach [4]. This is necessary because treatments aimed at the preservation of cultural heritage must meet specific requirements which make the simultaneous observation of various parameters necessary [16].

Many of these studies rely on discussions of spectroscopic data through visual and qualitative comparisons, leading to partial and scattered results without a systematic organisation [4]. The aim of this

* Corresponding author.
E-mail address: barbara.giussani@uninsubria.it (B. Giussani).

https://doi.org/10.1016/j.microc.2025.112971
Received 20 November 2024; Received in revised form 3 February 2025; Accepted 4 February 2025
Available online 6 February 2025

work is to propose a method that facilitates the study of ageing processes by leveraging chemometrics. Chemometrics serves as a valuable tool for highlighting differences in coatings over time and for discerning the individual contributions of the formulation components throughout the ageing process. It has demonstrated its effectiveness in various areas of cultural heritage, where inherently multivariate techniques are frequently employed for analysis [17].

The data were collected during the accelerated artificial solar light ageing of Paraloid® B44-based coatings prepared by casting solutions also containing a non-toxic corrosion inhibitor (in an effort to increasingly adhere to the principles of green chemistry) and a light stabilizer. Two types of corrosion inhibitors and two types of light stabilizers were selected. While the concentration of the corrosion inhibitors varied among the formulations, the concentration of Paraloid® B44 and the stabilizer remained constant, resulting in a total of twenty-one formulations (Table 1). Their stability over time was assessed by accelerated artificial solar light ageing and monitored at specific intervals to observe decay phenomena.

Fourier Transformed-Infrared Spectroscopy and UV–Vis spectroscopy were used to monitor the aging process, both using benchtop and portable spectrometers. It is worth noting that these techniques can be applied to real samples without specific pretreatment, thereby avoiding the use and waste of reagents. The analysis itself does not require chemicals. Additionally, these techniques are potentially portable, eliminating costs and waste associated with sample transportation and storage and reducing energy usage. All these factors make these techniques more aligned with the principles of green chemistry compared to others.

In this article, we present a method for laboratory studies that allows for an objective comparison of different coating formulations while remaining simple and easy to interpret. This approach also facilitates the application of the same methodology to real samples in real working conditions, enabling the use of techniques—preferably portable and in line with the principles of green analytical chemistry—to develop models for monitoring the effectiveness of protective treatments over time. The proposed method is based on the well-established technique of Principal Component Analysis (PCA) [18–20]. PCA has the powerful ability to extract relevant information from data while providing easily interpretable visual results. Here, we will leverage the strengths of spectroscopic techniques, including the ability to analyse samples non-invasively, combined with PCA (see [17] and reference therein and [21]).

2. Materials and methods

2.1. Samples

For this research, a set of 21 samples were prepared, following the scheme reported in Fig. 1. The coating formulation consists of an acrylic resin, Paraloid ® B44 (ethyl acrylate/methyl methacrylate copolymer, with methyl methacrylate > 50 %) purchased from Sinopia s.a.s., in solution with a combination of a corrosion inhibitor and a light stabiliser. Two types of corrosion inhibitors have been investigated: 5-mercapto-1-pheniltetrazole (MPT), purchased from Alfa Aesar and 2-amino-5-ethyl-1,3,4-thiadiazole (AEDTA) purchased from Sigma Aldrich. Two stabilizers were chosen based on their different mechanisms of action: Tinuvin® 312 (TIN312 in the text), ethanediamide N-(2-ethoxyphenil)-N'-(2-ethylphenil), and Tinuvin® 5050 (TIN5050 in the text), a mixture of 2-(2-hydroxyphenyl) benzotriazole and a HALS-Hindered Amine Light Stabilizer (the structure is unknown) obtained from BASF. The solvent used to solubilize the various components and prepare the coatings is 1-methoxy-2-propanol purchased from Sigma Aldrich.

The coatings were aged for 1000 h in a Q-Sun Xe-1 Xenon Test Chamber (Q-Lab Corporation, UK) at a constant temperature of 50 °C, irradiance set at 0.68 W/m^2 at 340 nm and Daylight Q filter (cut-on at 295 nm), simulating exposure to direct sunlight (usually, Xenon arc lamps may accelerate exposure up to 50 times natural conditions − 1000 h in an accelerated test might correspond to 1–4 years of natural exposure in a sunny weather with 250–300 sunny days per year). During ageing, the coatings were regularly monitored by a multi-analytical approach, whose outcomes have been the starting point for this work [10]. Indeed, the results of portable spectrophotometer measurements, UV–Vis and FTIR spectroscopy have been analysed using chemometrics.

For each analysis, a different type of support and coating application method was used. For UV–Vis the coatings were applied on quartz slides using a pipette, ensuring that the thickness was consistent across all samples. For FTIR analyses, silicon wafers were used, with the coatings applied in a controlled manner to ensure maximum reproducibility and consistency in the results. In particular, the thickness of the coatings was monitored to ensure that the absorbance of the most intense peak was between 0.7 and 1. For portable spectrophotometer measurements, a white tile was used, and the coatings were applied with a brush using two strokes in the same direction. This application protocol serves as a reasonable model for actual in situ application conditions.

Table 1
Different formulations of the coatings involved in the study.

Composition (wt%)		B44	AEDTA	MPT	TIN312	TIN5050	1-methoxy-2-propanol
Samples	**B44**	10	/	/	/	/	90
	B44 TIN312	10	/	/	0.3	/	89.7
	B44 TIN5050	10	/	/	/	0.3	89.7
	B44 1 % MPT	10	/	1	/	/	89
	B44 0.5 % MPT	10	/	0.5	/	/	89.5
	B44 0.1 % MPT	10	/	0.1	/	/	89.9
	B44 1 % MPT TIN312	10	/	1	0.3	/	88.7
	B44 0.5 % MPT TIN312	10	/	0.5	0.3	/	89.2
	B44 0.1 % MPT TIN312	10	/	0.1	0.3	/	89.6
	B44 1 % MPT TIN5050	10	/	1	/	0.3	88.7
	B44 0.5 % MPT TIN5050	10	/	0.5	/	0.3	89.2
	B44 0.1 % MPT TIN5050	10	/	0.1	/	0.3	89.6
	B44 1 % AEDTA	10	1	/	/	/	89
	B44 0.5 % AEDTA	10	0.5	/	/	/	89.5
	B44 0.1 % AEDTA	10	0.1	/	/	/	89.9
	B44 1 % AEDTA TIN312	10	1	/	0.3	/	88.7
	B44 0.5 % AEDTA TIN312	10	0.5	/	0.3	/	89.2
	B44 0.1 % AEDTA TIN312	10	0.1	/	0.3	/	89.6
	B44 1 % AEDTA TIN5050	10	1	/	/	0.3	88.7
	B44 0.5 % AEDTA TIN5050	10	0.5	/	/	0.3	89.2
	B44 0.1 % AEDTA TIN5050	10	0.1	/	/	0.3	89.6

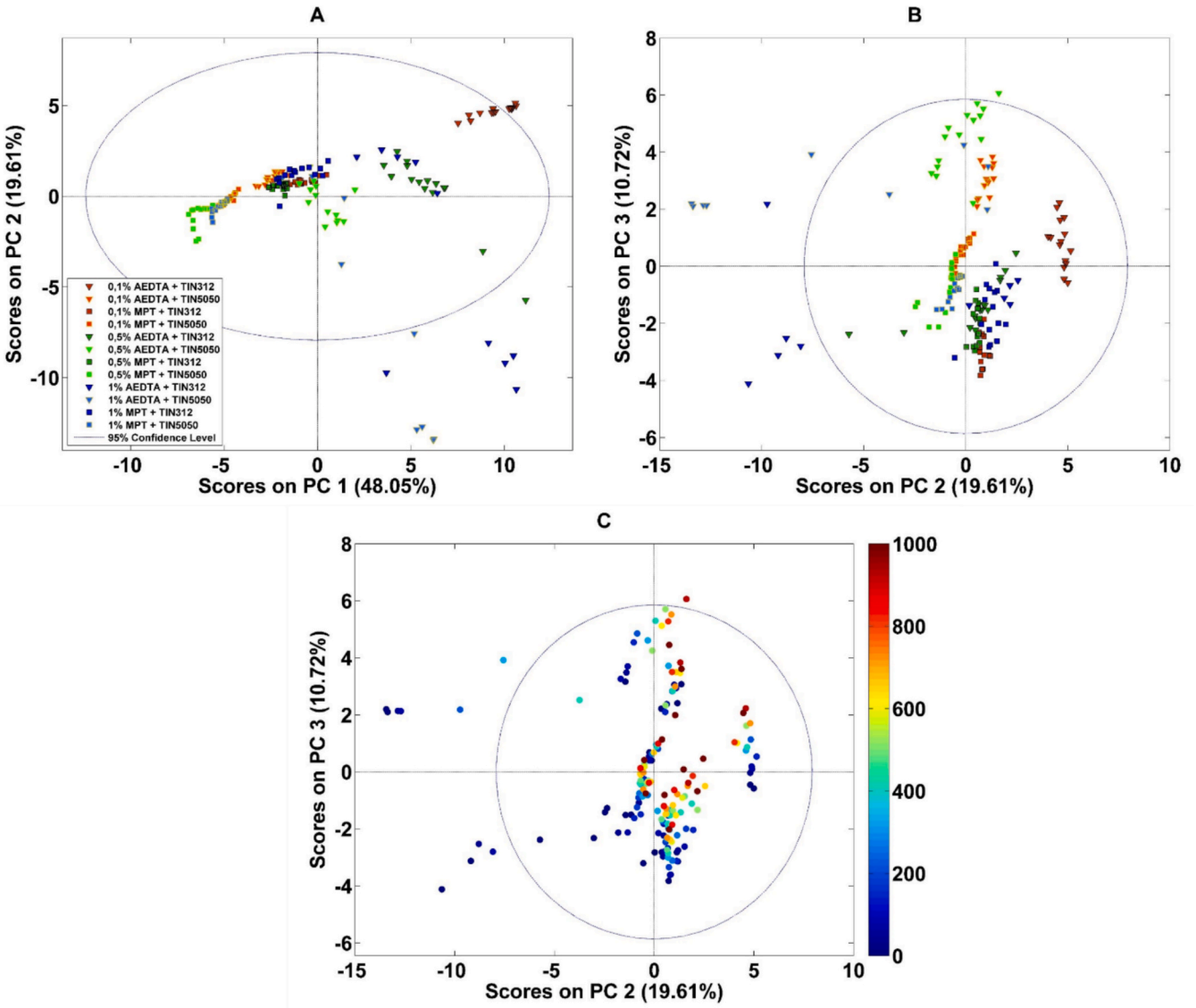

Fig. 1. Score plot PC1 vs PC2 (A) and PC2 vs PC3 (B-C) of the model built with all the studied formulations. Coatings with AEDTA are indicated by a triangular icon, while those with MPT are marked with a square icon. Formulations with a concentration of 0.1 % w/w of corrosion inhibitor and Tinuvin 312 are colored dark red with black border, while those with the same concentration of inhibitor but with Tinuvin 5050 are orange with yellow border. The ones with a concentration of 0.5 % w/w of corrosion inhibitor and Tinuvin 312 are colored dark green with black border, while those with Tinuvin 5050 are light green with yellow border. Formulations with a concentration of 1 % w/w of corrosion inhibitor and Tinuvin 312 are colored dark blue with black border, while those with Tinuvin 5050 are light blue with yellow border. Graph C describes the same samples over time: red colour represents 1000 h of ageing; blue colour represents time zero. (For interpretation of the references to color in this figure legend, the reader is referred to the web version of this article.)

2.2. Experimental plan

The samples were monitored through the three spectroscopic techniques mentioned above and divided into four groups due to spatial constraints inside the ageing chamber. Here, in Table 2, all the measurements made during ageing are reported.

2.3. Characterization

2.3.1. Fourier Transform Infrared spectroscopy (FTIR)

All coatings were applied on silicon supports and analysed in transmission mode with a Perkin Elmer Spectrum 100 spectrometer equipped with a DTS detector. Each analysis was performed by carrying out 16 scans in a range from 450 cm^{-1} to 4500 cm^{-1}, with a resolution of 4 cm^{-1}. A single analysis was performed for each sample.

2.3.2. Portable UV spectroscopy

UV spectra were recorded from 360 nm to 700 nm. Thin coatings were applied by brush on a white tile and analysed by a Portable Spectrophotometer CM-700d KONICA Minolta in SCI (Specular Component Included) mode. For each mock-up, a total of 15 measurements (5 measurement points, 3 measurements for each point) were acquired.

2.3.3. Benchtop UV–VIS spectroscopy

The UV–Vis spectra were acquired using a PerkinElmer Lambda 25 UV/vis spectrometer (Waltham, MA, USA) from 200 nm to 400 nm. Coatings were applied on quartz slide so that the extinction values did not exceed A = 1. A single analysis was performed for each sample.

2.4. Principal Component analysis (PCA)

Data treatment has been carried out using PLS Tollbox 9.2.1 running

Table 2
Experimental plan.

	Group 1	Group 2	Group 3	Group 4
	B44 0.5 % AEDTA		**B44**	**B44 1 % MPT TIN312**
	B44 0.1 % AEDTA		**B44 TIN312**	**B44 0.5 % MPT TIN312**
	B44 0.5 % AEDTA TIN312		**B44 TIN5050**	**B44 0.1 % MPT TIN312**
	B44 0.1 % AEDTA TIN312	**B44 1 % AEDTA**	**B44 0.5 % MPT**	**B44 1 % MPT TIN5050**
	B44 0.5 % AEDTA TIN5050	**B44 1 % AEDTA TIN312**	**B44 1 % MPT**	**B44 0.5 % MPT TIN5050**
	B44 0.1 % AEDTA TIN5050	**B44 1 % AEDTA TIN5050**	**B44 0.1 % MPT**	**B44 0.1 % MPT TIN5050**
t [h]	0	0	0	0
	24	24	24	48
	48	48	48	96
	70	72	72	168
	91	144	144	216
	163	216	192	264
	227	307	240	336
	327	402	312	384
	427	502	360	432
	520	661	408	528
	620	1000	480	600
	720		576	696
	812		648	768
	912		720	864
	1000		840	932
			1000	1000

under Matlab environment.

Spectra of coatings were organized in matrices, with wavelengths as columns and samples analysed at different times as rows. Each sample was represented as the average of the spectra obtained from each technique. The rows represent samples characterized by the concentration of the corrosion inhibitor (0.1 %, 0.5 %, and 1 % of AEDTA or MPT) and the type of light stabilizer used (TIN312 or TIN5050). They were monitored ranging from 0 to 1000 h of the aging process as reported in Table 2.

Prior to PCA, spectra were pretreated to correct unwanted variations caused by noise, atmospheric interferences like CO_2, baseline shifts and scattering effect [22,23].

The FTIR spectra comprised 1869 variables covering the 399–3992 cm^{-1} range, but better results were obtained for FTIR spectra considering the range 460–3750 cm^{-1} and removing regions ascribable to CO_2 (2300–2400 cm^{-1}) and matrix interferences (615, 746, 856, 1150, 1150–1190 and 1739 cm^{-1}) – as reported in [24]. Savitsky-Golay first derivative (21pt window, second order polynomial for the AEDTA formulations; 11pt window, second order polynomial for the MPT formulations and for the multiple-class models), SNV and mean centering were applied to this dataset.

UV–Vis spectra recorded with the portable instrument included 39 variables spanning from 360 to 740 nm. Savitsky-Golay first derivative (7pt window, second order polynomial), and mean centering were applied before PCA modelling.

Concerning the benchtop UV–Vis data, the relevant information was found in the spectral region between 200 and 400 nm, therefore the rest of the spectrum was excluded from the calculations. Smoothing (31pt window), first derivative (second order polynomial, 9pt window) SNV and mean centering were applied before PCA calculation.

3. Results and discussion

In the following sections of the article, the results of the chemometric reprocessing of the spectroscopic data collected during the aging of the samples are presented. Principal Component Analysis has proven to be highly effective in monitoring color measurements performed on outdoor bronze patinas and protective coating systems on bronze coupons to assess natural weathering and cleaning effects [25]. However, in the methodology proposed here, the spectrum is used as is, without extracting specific features as was done in the cited study. PCA provides two main plots: the scores plot, which describes the samples, and the loadings plot, which, in the case of spectroscopic techniques, highlights the spectral regions most significant for distinguishing differences between the samples. The score plots are usually displayed in a two-dimensional form. Additionally, when useful, the scores of individual principal components are plotted over time to emphasise how the samples change throughout the ageing process. It is essential to emphasize that each model describes only the specific system under study and enables the assessment of whether the substrates conditions remain stable or evolve over time. Clear and straightforward graphs have been thus used to illustrate how the samples change over time, based on the information captured by each analytical technique.

3.1. Fourier Transform Infrared spectroscopy (FTIR)

The very first model constructed with the FTIR data included the entire spectra. However, the resulting PCA model (data not shown) did not reveal a clear time evolution trend. The loadings analysis indicated that this outcome was probably due to the stability of the polymer, which remained nearly unchanged during the accelerated aging in all the samples, while other compounds underwent changes [10]. To enhance the information concerning changes during aging, specific spectral regions (polymer signal) were excluded [23] and a new model was recalculated.

The PC1 vs. PC2 score plot (Fig. 1A) clearly shows that the samples are distributed in the space according to their formulation. It is worth noting that the score plot represents the projection of the samples in the principal component space. Samples that are close to each other are similar, while samples that are farther apart are different. In graphs A and B, the samples are color-coded and labelled according to the formulation, as indicated in the caption, while in graph C, the samples are color-coded according to aging hours (0–1000), as indicated by the colour bar shown in the image. The possibility of distinguishing formulations containing TIN5050 is significant as the absorption peaks of this light stabiliser are masked by those of other components, making the FTIR spectra of these coatings visually indistinguishable from each other. Using multivariate analysis, they are clearly identifiable in the graph.

A clear distinction emerges between two subgroups: the coatings with AEDTA at positive PC1 values (represented with triangles in the figure) and the coatings with MPT at more negative values of the same component (square icon). PC1 also differentiates the samples based on the concentration of AEDTA. Increasing concentrations of the corrosion

inhibitor (0.1 %, 0.5 %, and 1 %) are represented by red, green, and blue triangles, respectively. This trend is particularly noticeable in samples containing TIN5050: as the concentration of the corrosion inhibitor increases, the PC1 values shift toward the higher positive part of the axis.

Information concerning the evolution in time can be found in PC2 vs PC3 score plot (Fig. 1C), with blue representing 0 h and red corresponding to 1000 h of aging. PC3 captures the information regarding the time evolution of most samples, except for the coatings with 1 % AEDTA, which display a distinct behaviour. The changes over time could be attributed to the fact that both types of corrosion inhibitors volatilize, which is a known drawback of this category of inhibitors [26].

The above presented model encompasses all the information contained within the dataset. To facilitate a more structured analysis, a viable approach is to develop models restricted to specific categories of samples, thereby enabling the model to process one set of information at a time more effectively. The initial step involves creating two separate models based on the type of corrosion inhibitor: one model for samples containing AEDTA and another for those with MPT.

As an example, the score plot for the model with AEDTA-containing samples is presented (Fig. 2A – samples are shape and color-coded according with the composition). This model again distinctly differentiates the samples according to the type of light stabiliser, placing samples with TIN5050 at more positive PC1 values compared to those with TIN312. As shown in the plot (Fig. 2B – samples are color-coded according to aging hours (0–1000), as indicated by the colour bar shown in the image), the samples are also arranged according to their aging process, but the evolution follows distinct directions. For example, the sample containing 0.1 % AEDTA + TIN312 (represented by a dark red triangle) shifts from the upper left of the plot towards a lower right position as it ages, while samples with 0.5 % AEDTA + TIN312 (dark green triangle) evolve from a lower-left position to a higher-right one. These differing evolutionary directions indicate that these samples

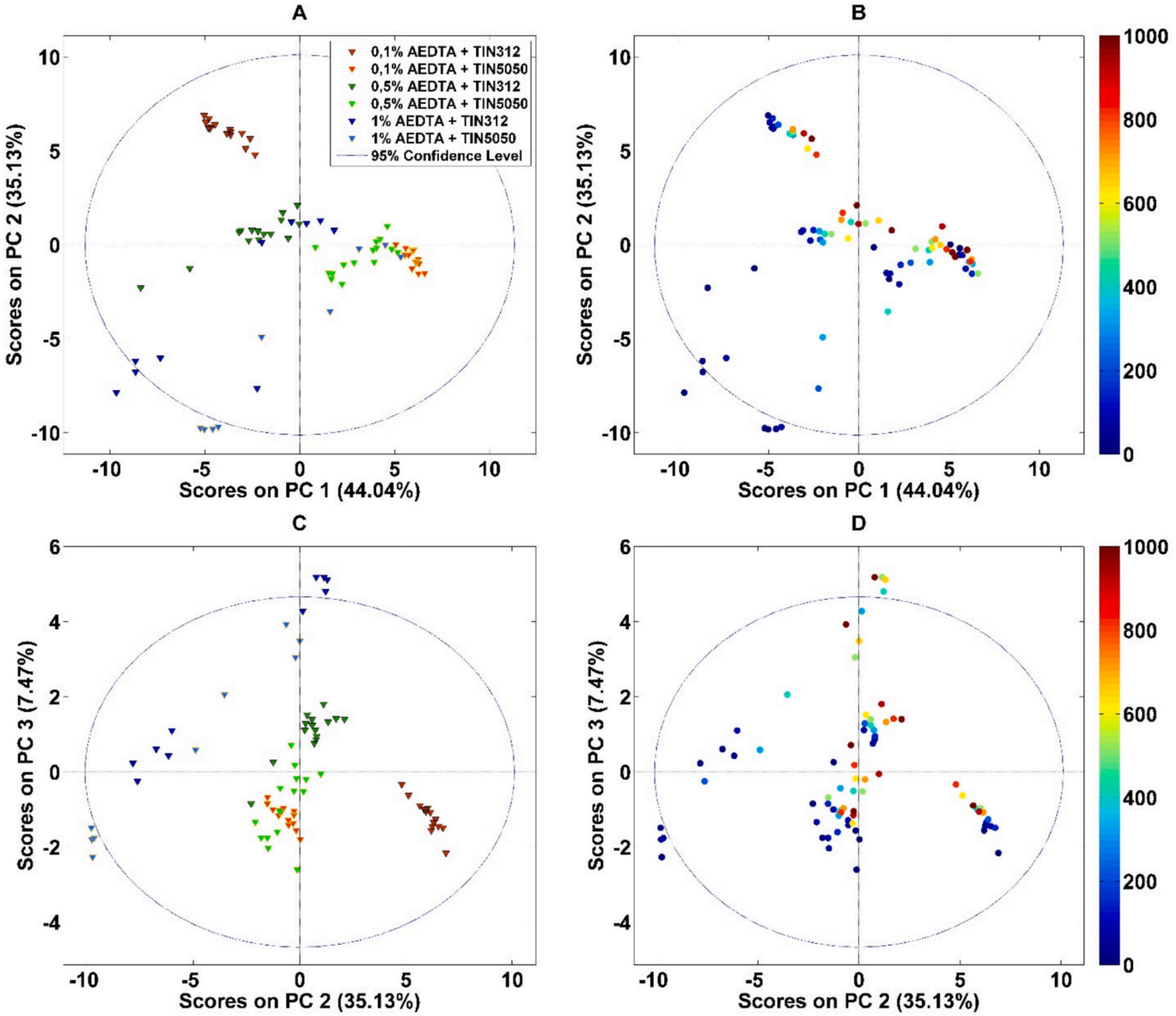

Fig. 2. Score plot PC1 vs PC2 (A-B) and PC2 vs PC3 (C-D) of the model built with AEDTA formulations. Formulations with a concentration of 0.1 % w/w of corrosion inhibitor and Tinuvin 312 are colored dark red with black border, while those with the same concentration of inhibitor but with Tinuvin 5050 are orange with yellow border. The ones with a concentration of 0.5 % w/w of corrosion inhibitor and Tinuvin 312 are colored dark green with black border, while those with Tinuvin 5050 are light green with yellow border. Formulations with a concentration of 1 % w/w of corrosion inhibitor and Tinuvin 312 are colored dark blue with black border, while those with Tinuvin 5050 are light blue with yellow border. Graphs B and D describe the same samples over time: red colour represents 1000 h of ageing; blue colour represents time zero. (For interpretation of the references to color in this figure legend, the reader is referred to the web version of this article.)

change differently over time depending on the concentrations of the corrosion inhibitors. PC3 (shown in Fig. 2C – samples are shape and color-coded according with the composition and 2D – samples are color-coded according to aging hours) again accounts for information concerning evolution over time (Fig. 2D).

It is worth noting that in a score plot, samples that are similar with respect to the variables used to describe them are positioned close together, while samples that are farther apart are more different. This means that the greater the distance between samples at time 0 and those at time 1000, the larger the differences observed in their Mid-Infrared (MIR) spectra. In other words, the more distant they are, the greater the changes that occurred during the artificial aging process. This is a significant result, as it enables a visual comparison of the outcomes of a controlled aging experiment, thereby facilitating the identification of the formulations most prone to aging and thus the selection of the more stable ones, for further development.

By delving into the analysis, it becomes feasible to model the evolution of individual samples to gain a deeper understanding of their trends. In this context, PCA should be conducted exclusively on samples belonging to a specific category, thereby allowing for the observation of differences at various stages of the controlled aging experiment. As an example, the results obtained from the models developed for the samples containing 0.5 % AEDTA and MPT are presented, utilizing the light stabilizer TIN5050 in one instance and TIN312 in another.

In this case, in Fig. 3 only the score values of PC1 for both models are presented. It is clearly demonstrated that the sample containing 0.5 % AEDTA + TIN312 undergoes a significant change during the initial phase of the accelerated aging, followed by minimal alterations after 100 h, exhibiting a slow yet continuous evolution. Conversely, the sample with TIN5050 experiences a more gradual change at the beginning, reaching a state of stability approximately around 500 h of artificial aging. In the case of samples containing 0.5 % MPT, a similar behaviour is observed. When TIN312 is present, there is a noticeable change at the beginning (though not as significant as that observed for AEDTA), followed by a gradual continuous change. Conversely, with TIN5050, a near plateau is reached after approximately 300 h. This approach allows for the rationalization and comparison of the evolutions of individual samples under investigation in a visual and intuitive manner.

Monitoring evolution in time with PCA is advantageous for several reasons. First, models proved to be capable of distinguishing between different formulations based on the type of inhibitor and light stabilizer, which is not a trivial task, given that some of these compounds exhibit overlapping signals in the MIR spectrum. Second, this approach enables a straightforward and intuitive comparison of the behaviours of these various protective coatings, identifying common or differing evolutionary directions over time, thereby facilitating informed decisions regarding the optimal formulation. Third, it allows for the monitoring of individual samples over time, providing insights into their evolution.

3.2. Portable UV spectroscopy

The analysis with portable UV spectrophotometer produced interesting results regarding the decay of light stabilisers and corrosion inhibitors.

As highlighted in Fig. 4, the difference between the two Tinuvin is clear: the symbols with the yellow border- namely the coatings with Tinuvin 5050- stay on the right while the ones with the black border are on the left. On PC1, the evolution with time of Tinuvin 5050-based formulations emerges, while on PC2, the temporal evolution of Tinuvin 312-based formulations and the difference between coatings with MPT or AEDTA can be seen. The evolutions, being almost orthogonal to each

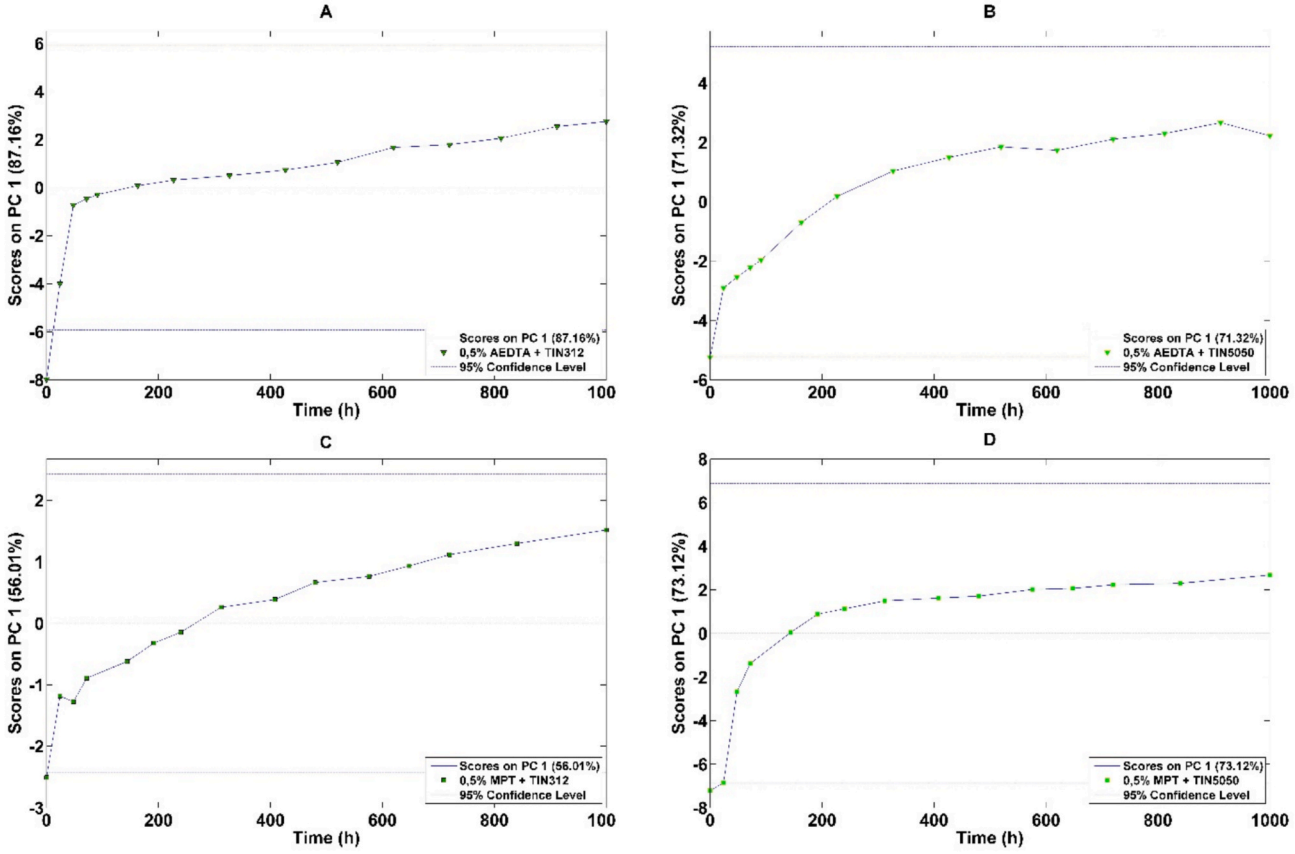

Fig. 3. Plot of the scores on PC1 versus time (hours) of 0.5 % w/w AEDTA, Tinuvin 312 (Graph A), 0.5 % AEDTA Tinuvin 5050 (Graph B), 0.5 % w/w MPT and Tinuvin 312 (graph C), 0.5 % w/w MPT and Tinuvin 5050 (Graph D).

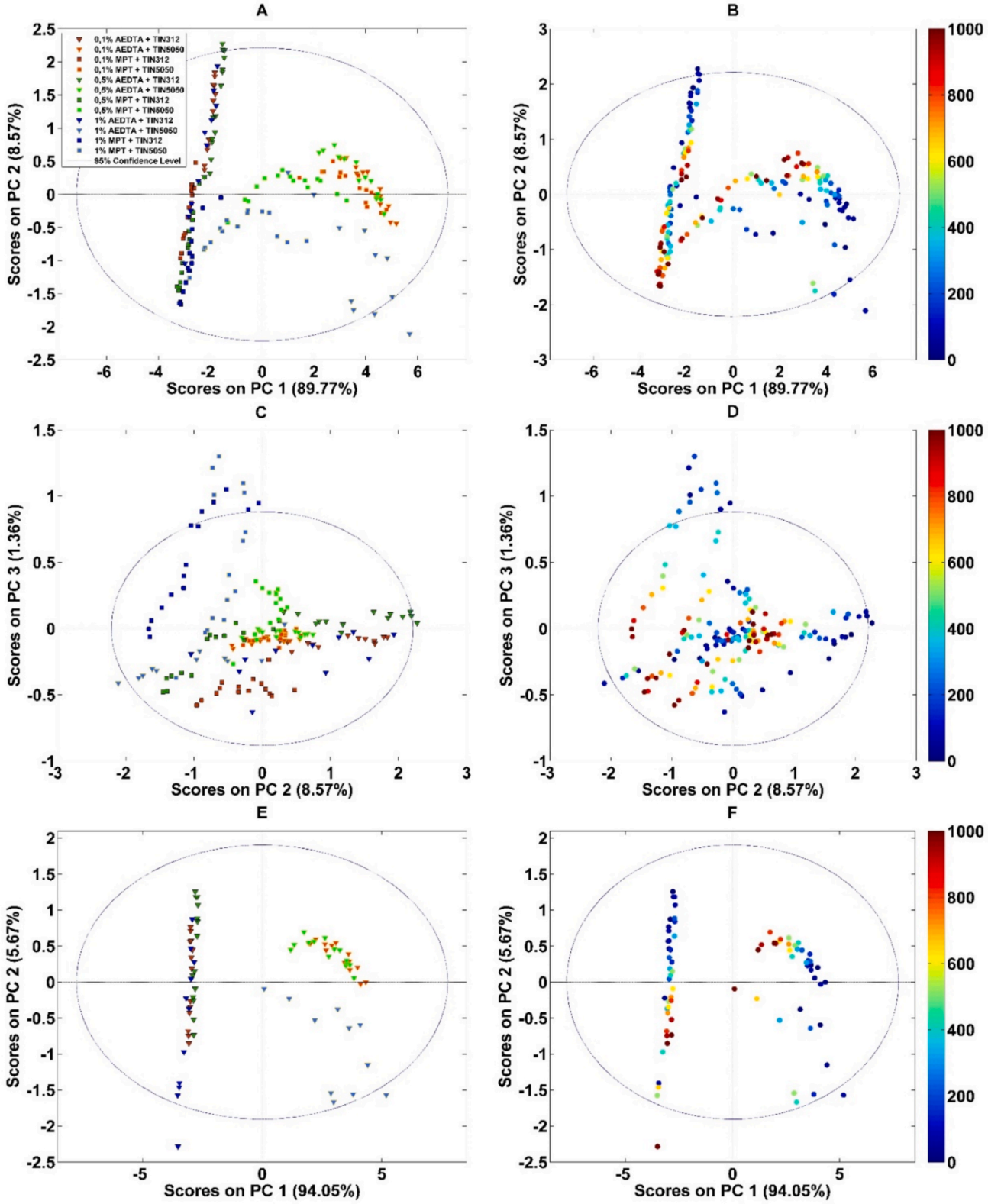

Fig. 4. Score plot PC1 vs PC2 (A-B), PC2 vs PC3 (C-D) of the model built with all formulations. Graph E and graph F are referred only to score plots PC1 vs PC2 of AEDTA coatings. Formulations with a concentration of 0.1 % w/w of corrosion inhibitor and Tinuvin 312 are colored dark red with black border, while those with the same concentration of inhibitor but with Tinuvin 5050 are orange with yellow border. The ones with a concentration of 0.5 % w/w of corrosion inhibitor and Tinuvin 312 are colored dark green with black border, while those with Tinuvin 5050 are light green with yellow border. Formulations with a concentration of 1 % w/w of corrosion inhibitor and Tinuvin 312 are colored dark blue with black border, while those with Tinuvin 5050 are light blue with yellow border. Graphs B, D and F describe the same samples over time: red colour represents 1000 h of ageing; blue colour represents time zero. (For interpretation of the references to color in this figure legend, the reader is referred to the web version of this article.)

other, suggest independent mechanisms of decay involving the light stabilizers, that are specific for the chemical classes they are in.

On PC2, an evolutionary direction can be identified, which, for almost all samples, moves from more positive PC2 values toward more negative ones. Samples that show greater distances between the starting point of the accelerated aging (0 h) and the final point (1000 h) are more different, indicating that accelerated aging has caused a more significant change in their composition. The PC2 versus PC3 plot highlights the time evolution of 1 % MPT-containing formulations on PC3. This could indicate that the direction of evolution over time, i.e., the decay of MPT, strongly depends on its concentration, as samples with the three MPT concentrations follow different evolutionary paths. In contrast, formulations containing AEDTA follow a single evolutionary direction. It is interesting to note also that the direction of evolution of 1 % MPT samples moves from more positive PC3 values toward values similar to those of the other samples. This could indicate that, after the aging process, the samples with 1 % MPT exhibit a chemical composition—detectable by the sensor used in this experiment—more akin to that of the samples with lower concentrations of the same chemical substance. In other words, it is as if the MPT concentration shifts from 1 % to values closer to those of the other samples, which contain 0.5 % and 0.1 %. This suggests that the coating decay is more pronounced at higher MPT concentrations, confirming what has already been demonstrated by Pellis and co-authors [10].

As before, to better rationalize the information contained in this graph, it is useful to create submodels by dividing the different categories of samples.

Fig. 4E and 4F present the score plot for the PCA model developed using samples containing AEDTA. The first principal component (PC1) accounts for the majority of the variance and effectively separates the samples based on the type of Tinuvin used. However, when the samples are color-coded according to the aging time, it becomes evident that those containing TIN5050 are arranged along PC1 in line with their evolution, progressing from time 0, located at more positive PC1 values, toward the centre of the model. In contrast, samples with TIN312 are organized according to their aging along PC2, which explains less than 6 % of the total information. This observation reinforces the notion that each light stabilizer follows its unique direction of change over time, with TIN5050 demonstrating more significant variations compared to TIN312, whose signal remains relatively stable [10]. It is crucial to recall that the results of a PCA depend on the chemical signals (the variables) used in its construction.

3.3. Benchtop UV spectroscopy

The benchtop spectrometer was thus used to confirm the results

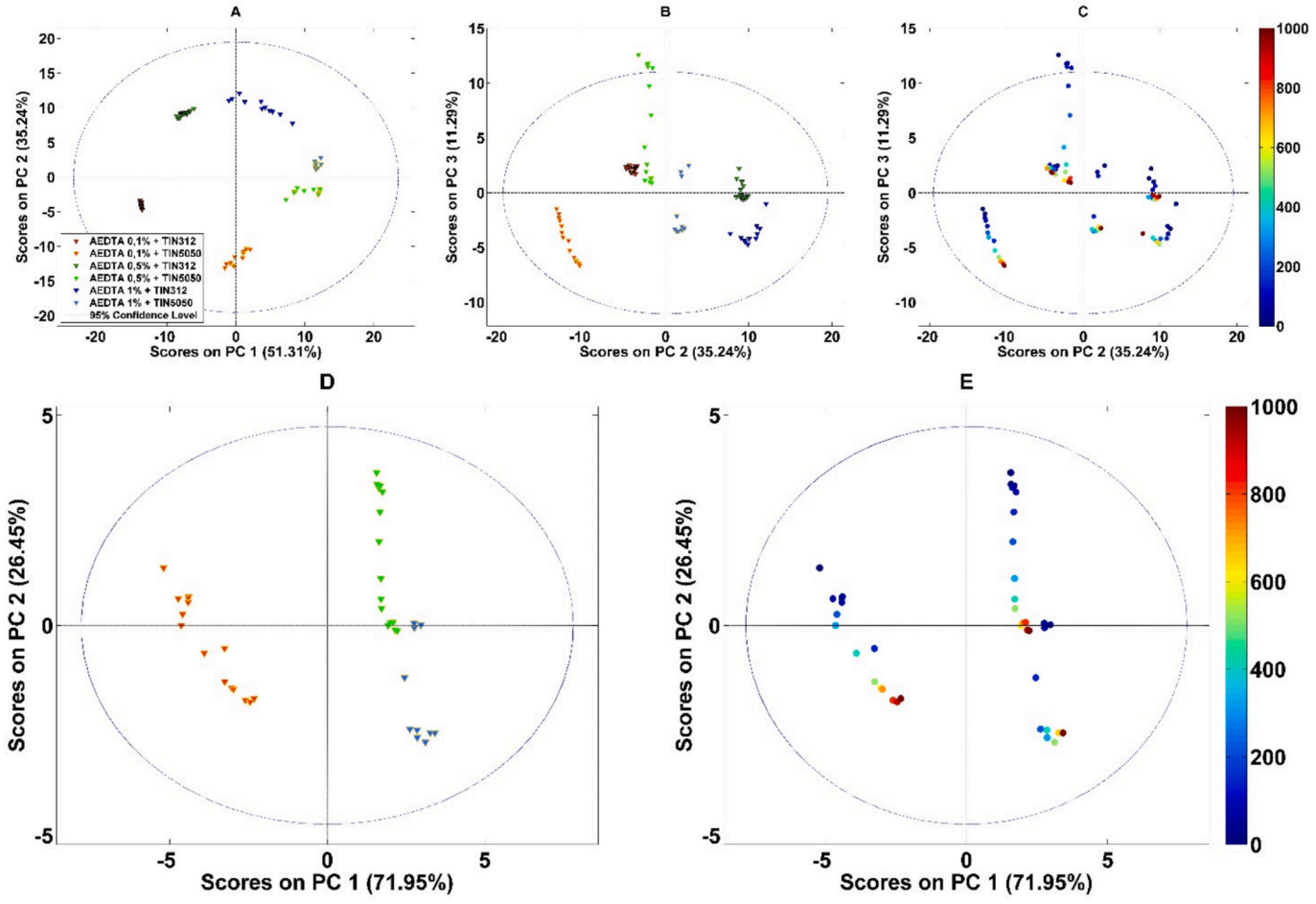

Fig. 5. Score plot PC1 vs PC2 (A) and PC2 vs PC3 (B-C) of the model built with AEDTA formulations. Graphs D and E refer only to AEDTA and Tinuvin 5050 coatings. Formulations with a concentration of 0.1 % w/w of corrosion inhibitor and Tinuvin 312 are colored dark red with black border, while those with the same concentration of inhibitor but with Tinuvin 5050 are orange. The ones with a concentration of 0.5 % w/w of corrosion inhibitor and Tinuvin 312 are colored dark green with black border, while those with Tinuvin 5050 are light green with yellow border. Formulations with a concentration of 1 % w/w of corrosion inhibitor and Tinuvin 312 are colored dark blue with black border, while those with Tinuvin 5050 are light blue with yellow border. Graphs C and E describe the same samples over time: red colour represents 1000 h of ageing; blue colour represents time zero. (For interpretation of the references to color in this figure legend, the reader is referred to the web version of this article.)

already obtained for the samples containing AEDTA, whose behaviour during accelerated aging proved to be more homogeneous across different AEDTA concentrations, and therefore more stable and easier to rationalize. The Principal Component Analysis performed on the data collected from the UV range measured by this instrument yields interesting insights (Fig. 5).

As we expected, the model is able to group the samples based on their chemical composition. Moreover, the model can also arrange the samples containing AEDTA according to its concentration: samples with lower concentrations of AEDTA are positioned in the low left quadrant, while those with higher concentrations are located in the high positive one. The model distinguishes also the presence of the light stabilizer: samples with TIN5050 are located in the lower right part of the graph, while samples containing TIN312 lie in the upper left part. Looking at PC3, it is possible to see that the samples are arranged based on time variability. What stands out most from this model is that the samples containing TIN5050 undergo greater changes over time compared to those containing TIN312, especially for samples containing low concentration levels of corrosion inhibitor. This agrees with results observed in the chemometric analysis of MIR data and also by py-GC/MS determination [10].

Further narrowing down the dataset, the model obtained for the samples with AEDTA and TIN5050 is presented. The information contained in the first axis, which represents the greatest variability, is the difference in the concentration of the corrosion inhibitor, while the second axis shows the evolution over time. It is clearly visible that samples with a low concentration of the anticorrosion additive evolve more significantly over time compared to samples with a high concentration of the same, according to the information that this instrument operating between 200 and 400 nm is capable of capturing. The models are therefore capable on the one hand to recognize the different formulations and on the other to visually represent their evolution over time, allowing for easy comparison.

4. Conclusions

Monitoring the evolution of coatings designed to protect metal artworks from corrosion is a challenging task for researchers. This article presents a non-destructive methodology based on spectroscopic techniques combined with chemometric analysis, offering straightforward interpretability. The simplicity of interpretation makes it an ideal approach for introducing professionals in cultural heritage and restoration to these methods. The proposed monitoring system, using principal component analysis, effectively distinguishes between different coatings and facilitates the interpretation of decay differences as the formulations age.

This method enables an easy and intuitive selection of optimal formulations using simple, interpretable two-dimensional graphs, allowing users to understand without needing expertise in spectra interpretation. The portable UV–Vis data indicated that MPT coatings are more prone to degradation, whereas benchtop UV–Vis analysis revealed that Tinuvin 5050 experiences more substantial changes over time. This complementary information, easily interpreted through the chemometric approach proposed, led to the selection of AEDTA and Tinuvin 312 as the optimal solution. The results obtained in this study confirm those of previous work, demonstrating that this approach is effective and robust for decay studies, and lay the foundation for the application of this innovative methodology in real-world cases. It is worth highlighting that this methodology can be similarly applied to the study of any type of coating, demonstrating its versatility and effectiveness across a wide range of applications—not only in cultural heritage preservation but also in various other fields.

CRediT authorship contribution statement

Giulia Pellis: Writing – original draft, Investigation, Data curation. **Maxim Tiburziano:** Visualization, Formal analysis. **Barbara Giussani:** Conceptualization, Supervision, Funding acquisition, Writing – review & editing. **Paola Letardi:** Conceptualization, Resources, Writing – review & editing. **Barbara Salvadori:** Funding acquisition, Methodology. **Antonio Sansonetti:** Methodology, Writing – review & editing. **Dominique Scalarone:** Funding acquisition, Project administration.

Declaration of competing interest

The authors declare that they have no known competing financial interests or personal relationships that could have appeared to influence the work reported in this paper.

Acknowledgements

This research was funded by Progetto di Ricerca di Interesse Nazionale PRIN 2022 “Innovative multi analytical Characterisation of the influence of pAtina-coating inteRaction on anti-corrosive propErties – InCARE” (Project code: 2022895PTX), funded by MUR and the European Union – Next Generation EU, M4.C2.1.1, CUP B53D23001230006.

G.P and D.S. acknowledge support from the Project CH4.0 under the MUR program “Dipartimenti di Eccellenza 2023-2027” (CUP: D13C22003520001).

Data availability

Data will be made available on request.

References

[1] P. Letardi, Testing New Coatings for Outdoor Bronze Monuments: A Methodological Overview, Coatings 11 (2021), https://doi.org/10.3390/coatings.
[2] B. Salvadori, A. Cagnini, M. Galeotti, S. Porcinai, S. Goidanich, A. Vicenzo, C. Celi, P. Frediani, L. Rosi, M. Frediani, et al., Traditional and Innovative Protective Coatings for Outdoor Bronze: Application and Performance Comparison, J. Appl. Polym. Sci. 135 (2018), https://doi.org/10.1002/app.46011.
[3] M.T. Molina, E. Cano, B. Ramírez-Barat, Testing Protective Coatings for Metal Conservation: The Influence of the Application Method, Herit. Sci. 11 (2023), https://doi.org/10.1186/s40494-023-00937-0.
[4] M.T. Molina, E. Cano, B. Ramírez-Barat, Protective Coatings for Metallic Heritage Conservation: A Review, J. Cult. Herit. 62 (2023) 99–113.
[5] G. Masi, C. Josse, J. Esvan, C. Chiavari, E. Bernardi, C. Martini, M.C. Bignozzi, C. Monticelli, F. Zanotto, A. Balbo, et al., Evaluation of the Protectiveness of an Organosilane Coating on Patinated Cu-Si-Mn Bronze for Contemporary Art, Prog. Org. Coat. 127 (2019) 286–299, https://doi.org/10.1016/j.porgcoat.2018.11.027.
[6] E. Bescher, J.D. Mackenzie, Sol-Gel Coatings for the Protection of Brass and Bronze, J. Solgel. Sci. Technol. 26 (2003) 1223–1226, https://doi.org/10.1023/A:1020724605851.
[7] C. Chiavari, A. Balbo, E. Bernardi, C. Martini, F. Zanotto, I. Vassura, M.C. Bignozzi, C. Monticelli, Organosilane Coatings Applied on Bronze: Influence of UV Radiation and Thermal Cycles on the Protectiveness, Prog. Org. Coat. 82 (2015) 91–100, https://doi.org/10.1016/j.porgcoat.2015.01.017.
[8] T. Kosec, L. Škrlep, E. Švara Fabjan, A. Sever Škapin, G. Masi, E. Bernardi, C. Chiavari, C. Josse, J. Esvan, L. Robbiola, Development of Multi-Component Fluoropolymer Based Coating on Simulated Outdoor Patina on Quaternary Bronze, Prog. Org. Coat. 131 (2019) 27–35, https://doi.org/10.1016/j.porgcoat.2019.01.040.
[9] G. Bierwagen, T.J. Shedlosky, K. Stanek, Developing and Testing a New Generation of Protective Coatings for Outdoor Bronze Sculpture, Proceedings of the Progress in Organic Coatings 48 (December 2003) 289–296.
[10] G. Pellis, B. Giussani, P. Letardi, T. Poli, P. Rizzi, B. Salvadori, A. Sansonetti, D. Scalarone, Improvement in the Sustainability and Stability of Acrylic Protective Coatings for Outdoor Bronze Artworks, Polym. Degrad. Stab. 218 (2023), https://doi.org/10.1016/j.polymdegradstab.2023.110575.
[11] T. Kosec, H.O. Ćurković, A. Legat, Investigation of the Corrosion Protection of Chemically and Electrochemically Formed Patinas on Recent Bronze, Electrochim. Acta 56 (2010) 722–731, https://doi.org/10.1016/j.electacta.2010.09.093.
[12] T. Kosec, A. Legat, E. Stupnišek-Lisac, Improvement of Corrosion Stability of Patinated Bronze, in: Corrosion of Archaeological and Heritage Artefacts EFC 45, 2017, pp. 327–333.
[13] R. Bostan, S. Varvara, L. Găină, T. Petrisor, L.M. Mureşan, Protective Effect of Inhibitor-Containing Nitrocellulose Lacquer on Artificially Patinated Bronze, Prog. Org. Coat. 111 (2017) 416–427, https://doi.org/10.1016/j.porgcoat.2016.08.004.
[14] D.A. Jáuregui-Gónzalez, F.J. Rodríguez-Gómez, J. Contreras-Vargas, P. Roncagliolo-Barrera, M. López-Arriaga, Influence of the Application and Preparation of Wax Coatings on Artificially Patinated Bronze Surfaces, METAL (2016) 170–177.

[15] N. Swartz, T.L. Clare, On the Protective Nature of Wax Coatings for Culturally Significant Outdoor Metalworks: Microstructural Flaws, Oxidative Changes, and Barrier Properties, J. Am. Inst. Conserv. 54 (2015) 181–201, https://doi.org/10.1179/1945233015Y.0000000012.
[16] E. Cano, D. Lafuente, D.M. Bastidas, Use of EIS for the Evaluation of the Protective Properties of Coatings for Metallic Cultural Heritage: A Review, J. Solid State Electrochem. 14 (2010) 381–391.
[17] J. Riu, B. Giussani, Analytical Chemistry Meets Art: The Transformative Role of Chemometrics in Cultural Heritage Preservation, Chemom. Intell. Lab. Syst. 247 (2024), https://doi.org/10.1016/j.chemolab.2024.105095.
[18] Esbensen, K.H.; Geladi, P. Principal Component Analysis: Concept, Geometrical Interpretation, Mathematical Background, Algorithms, History, Practice. In: S. Brown, R. Tauler, B. Walczak (Eds), Comprehensive chemometrics: Chemical and biochemical data analysis, Elsevier, 2020; Vol. 2 ISBN 0444641653.
[19] Mardia K. V.; Kent J.T.; Bibby J.M. *Multivariate Analysis*; Academic Press, London, 1989; ISBN 0323-3847.
[20] Jackson, J.E. *A User's Guide to Principal Components*; John Wiley & Sons, 2005; ISBN 0471725323.
[21] H. Xuesong, C. Pu, L. Jingyan, X. Yupeng, L. Dan, C. Xiaoli, Commentary on the review articles of spectroscopy technology combined with chemometrics in the last three years, Appl. Spectrosc. Rev. 59 (4) (2023) 423–482, https://doi.org/10.1080/05704928.2023.2204946.
[22] Å. Rinnan, F. Van Den Berg, S.B. Engelsen, Review of the Most Common Pre-Processing Techniques for near-Infrared Spectra, Trends Anal. Chem. 28 (2009) 1201–1222.
[23] Å. Rinnan, L. Norgaard, F. van den Berg, J. Thygesen, R. Bro, S.B. Engelsen, Data Pre-Processing, in: D.-W. Sun (Ed.), Infrared Spectroscopy for Food Quality Analysis and Control, Elsevier, Amsterdam, 2008, pp. 29–50.
[24] M. Haris, S. Kathiresan, S. Mohan, FT-IR and FT-Raman Spectra and Normal Coordinate Analysis of Poly Methyl Methacrylate, Der Pharma Chemica 2 (2010) 316–323.
[25] G. Luciano, R. Leardi, P. Letardi, Principal component analysis of colour measurements of patinas and coating systems for outdoor bronze monuments, J Cult Herit 10 (2009) 331–337, https://doi.org/10.1016/j.culher.2008.10.004.
[26] M. Nawaz, S. Ahmad, M.G. Taryba, M.F. Montemor, R. Kahraman, R.A. Shakoor, Improvement in Inhibition Performance of Anti-Corrosion Coatings Using Polyolefin Matrix Embedded with Modified TiO2 Nanoparticles, Prog. Org. Coat. 195 (2024), https://doi.org/10.1016/j.porgcoat.2024.108659.